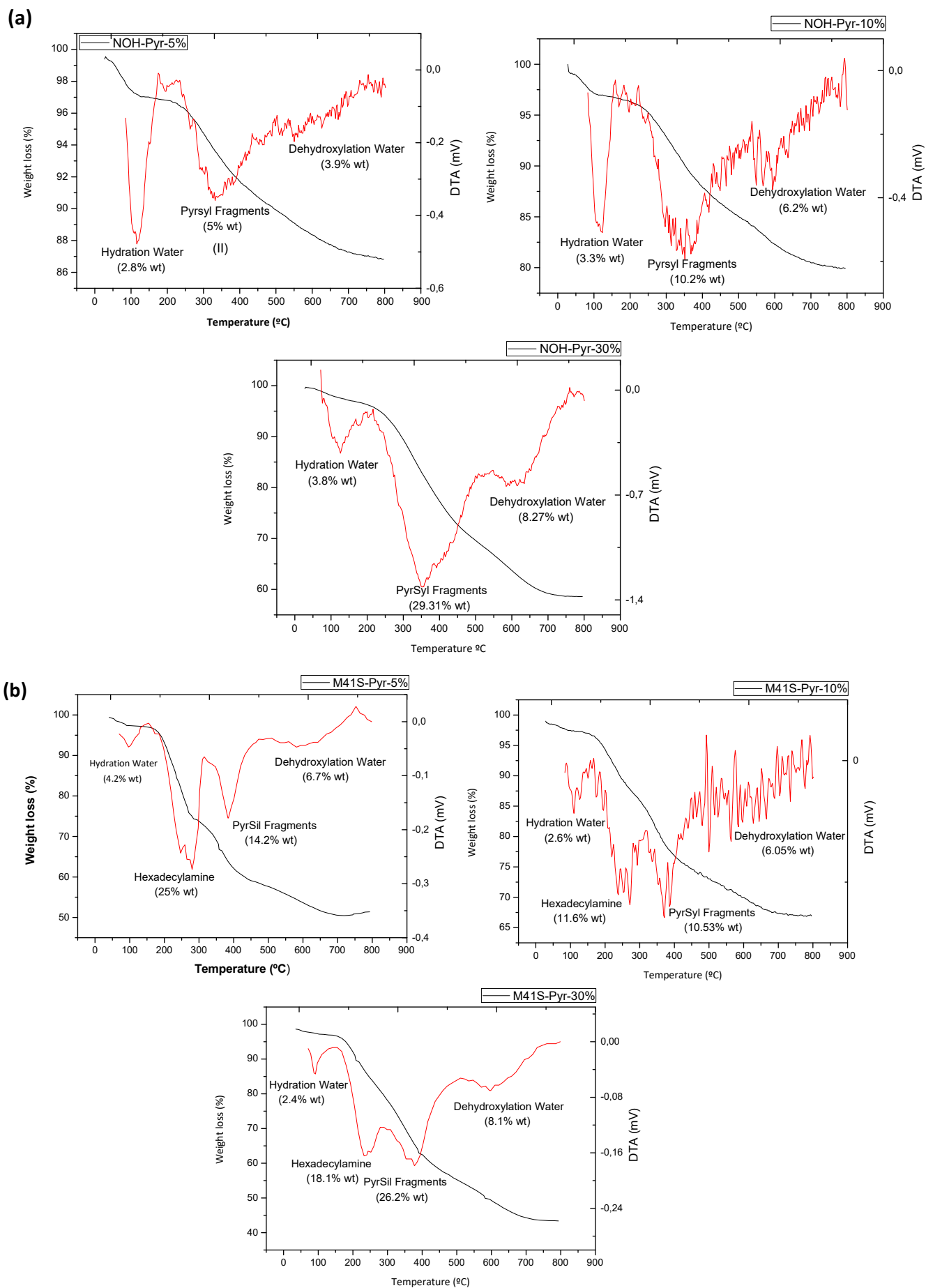


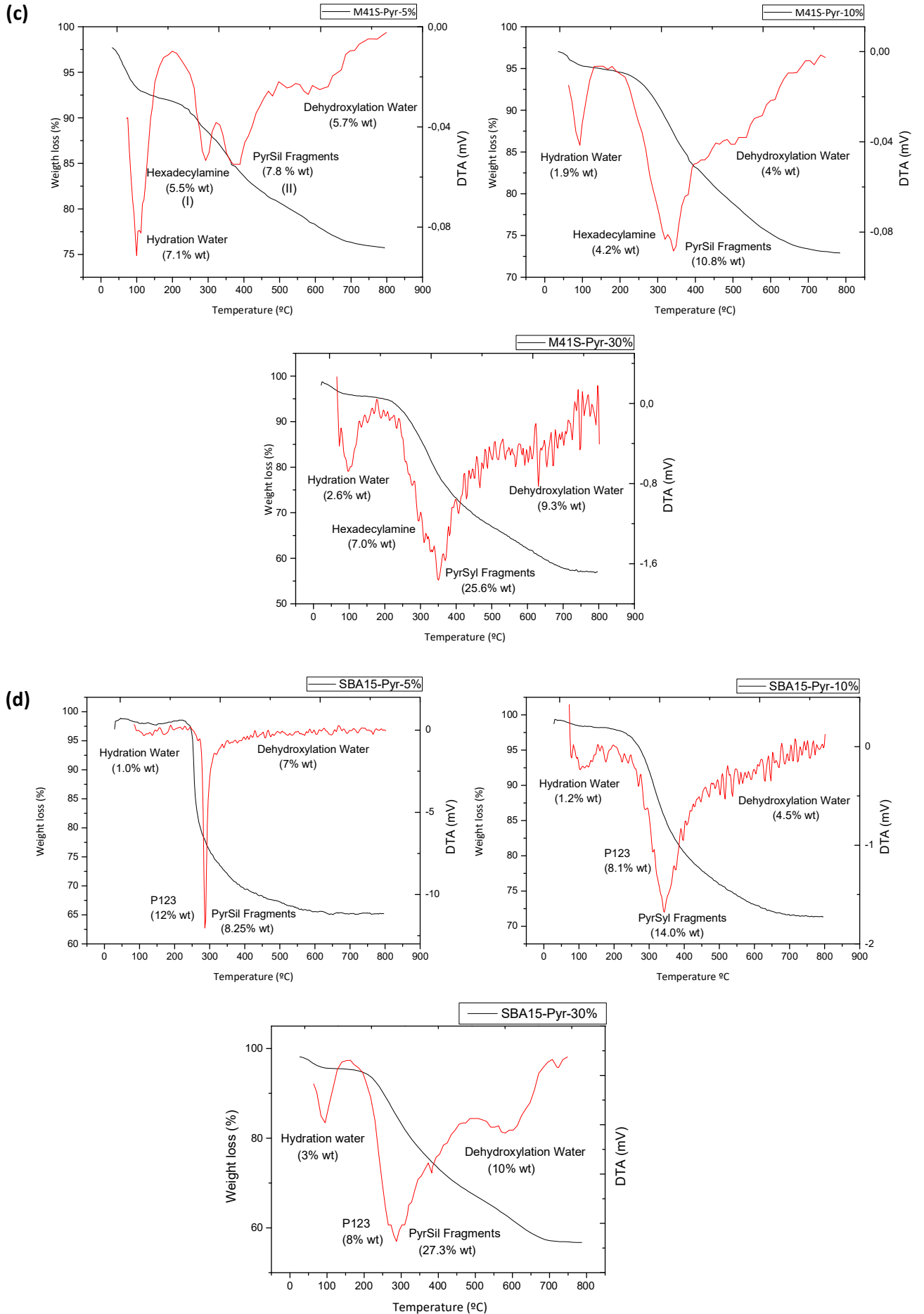
Influence of the Framework Topology on the Reactivity of Chiral Pyrrolidine Units Inserted in Different Porous Organosilicas

Sebastián Llopis, Alexandra Velty and Urbano Díaz *

¹ Instituto de Tecnología Química, Universitat Politècnica de València-Consejo Superior de Investigaciones Científicas, Avenida de los Naranjos s/n, E-46022 Valencia, Spain

* Correspondence: udiaz@itq.upv.es; Tel.: +34963877811





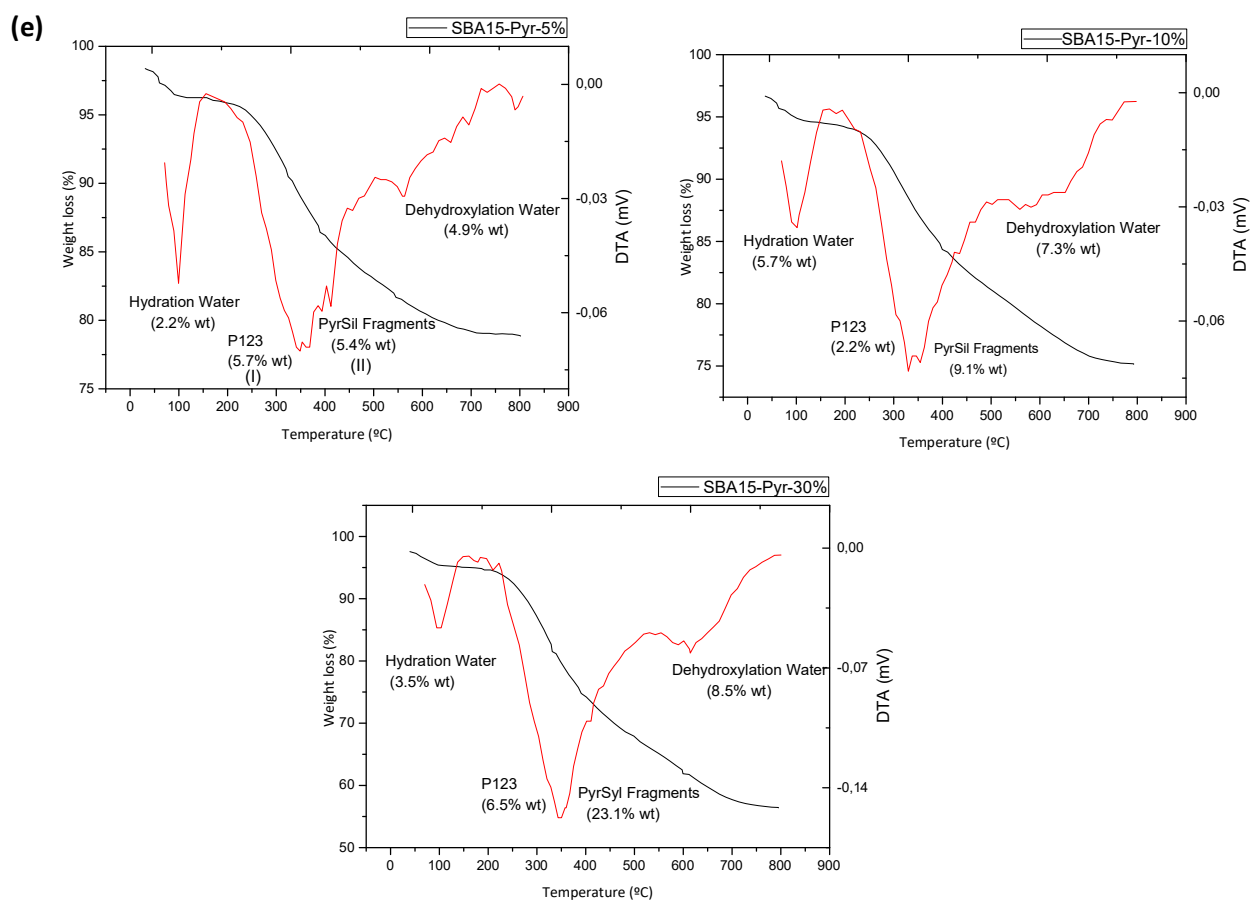
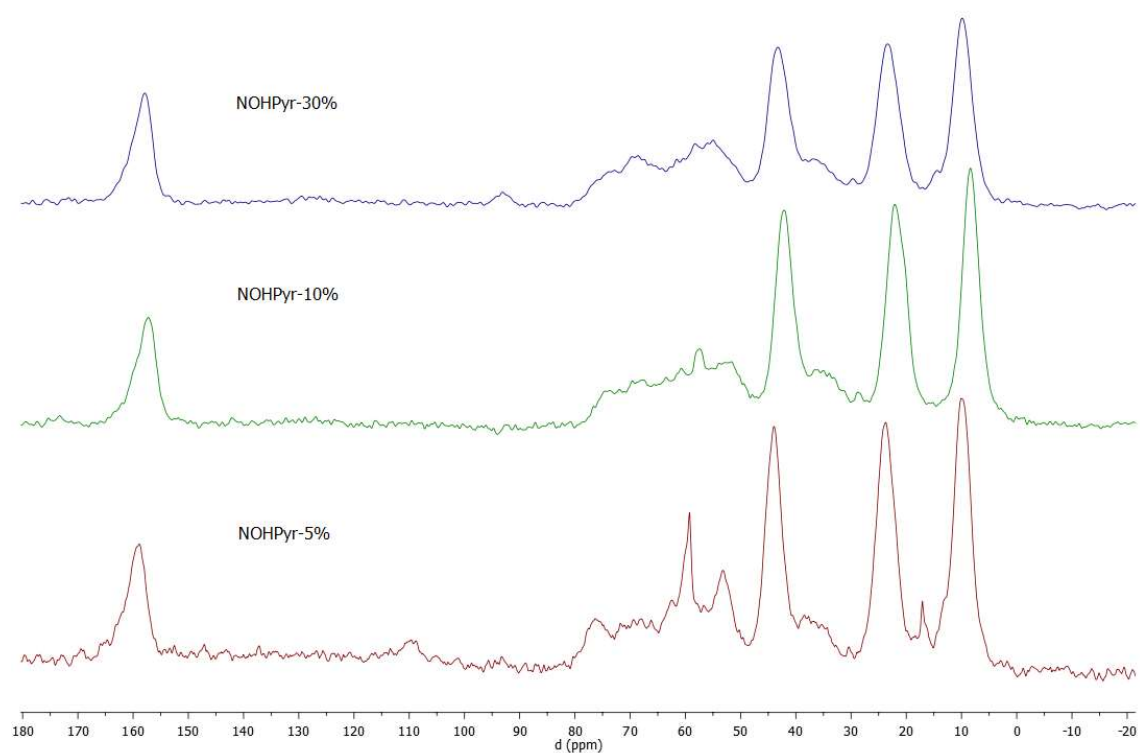
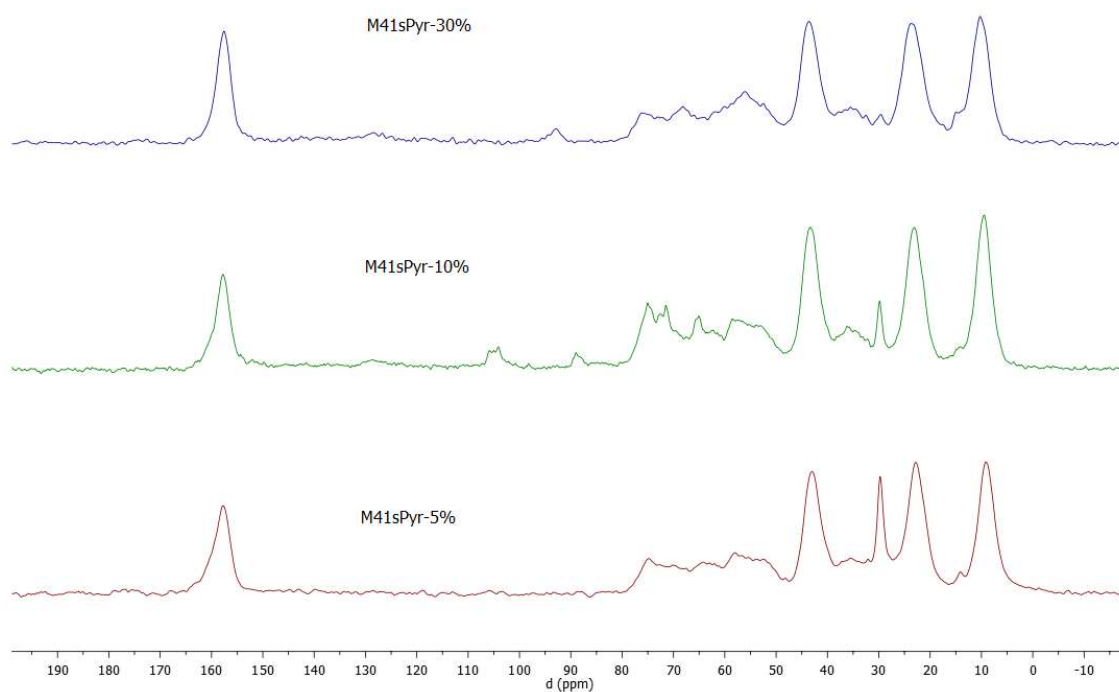


Figure S1. Thermogravimetical curves (TGA) and corresponding derivatives (DTA) of (a) NOH-Pyr, (b) as-synthesized M41S-Pyr, (c) extracted M41S-Pyr, (d) as-synthesized SBA-15-Pyr and (e) extracted SBA-15-Pyr materials with different content of bis-silylated pyrrolidine fragments.

a)



b)



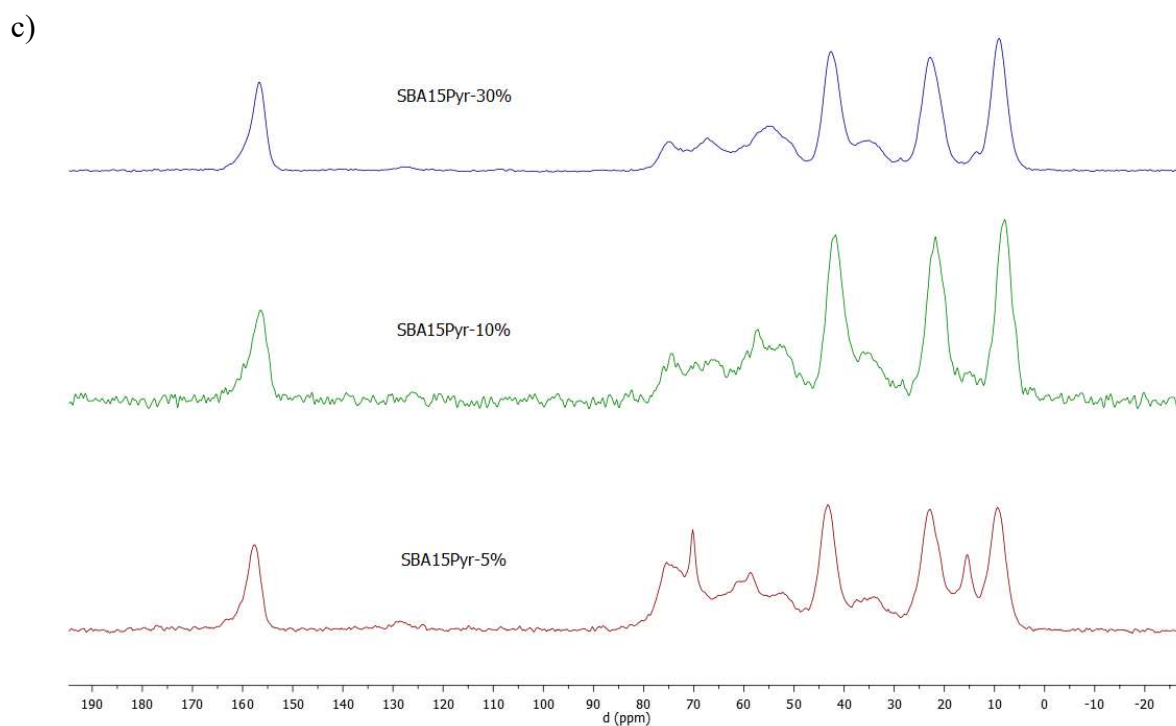


Figure S2. ^{13}C MAS NMR spectra of (a) NOH-Pyr, (b) M41S-Pyr and (c) SBA-15-Pyr materials containing different content of bis-silylated pyrrolidine fragments, obtained after extraction processes.

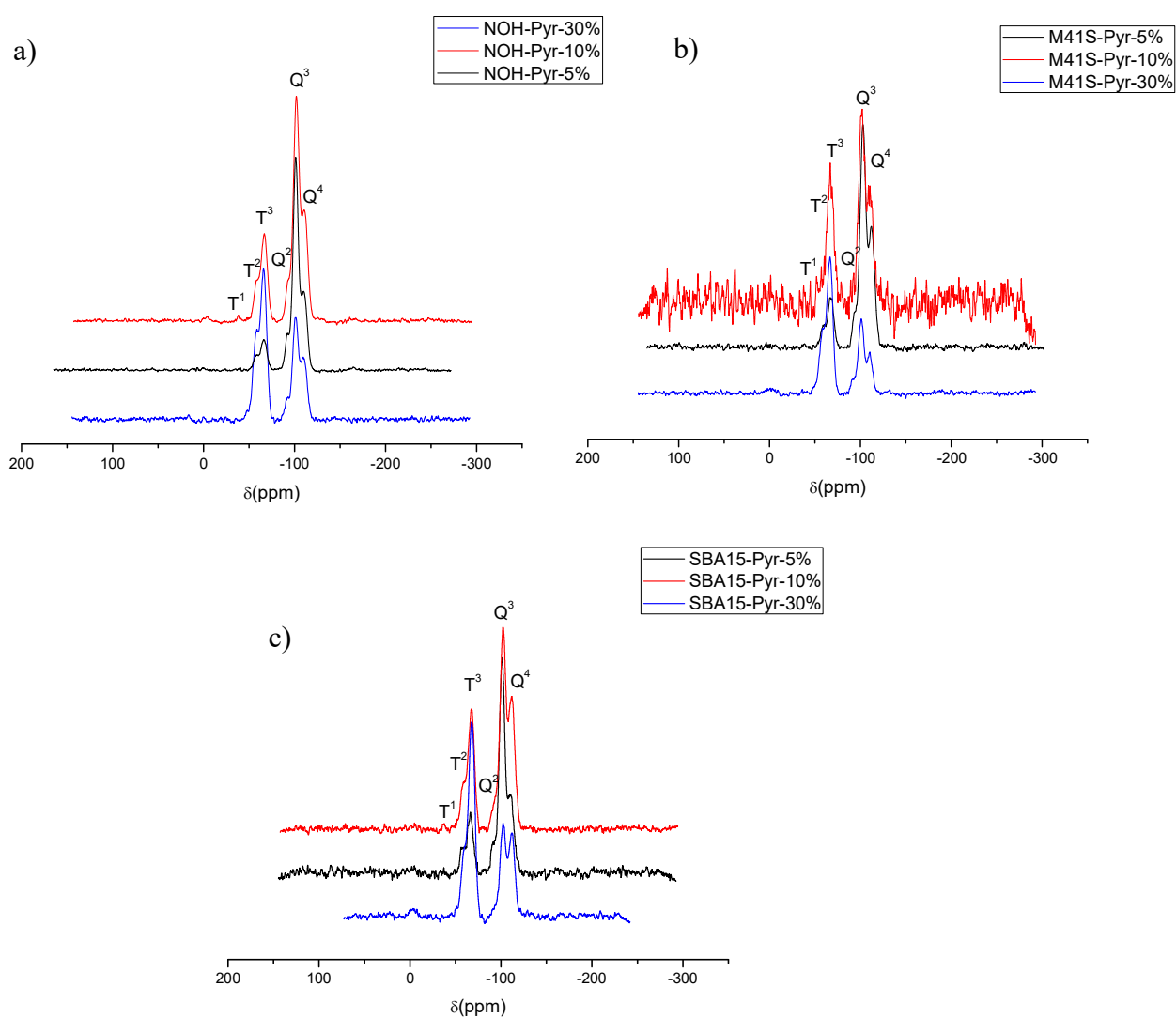


Figure S3. ^{29}Si CP/MAS NMR spectra of (a) NOH-Pyr, (b) M41S-Pyr and (c) SBA-15-Pyr materials, containing different content of bis-silylated pyrrolidine fragments, obtained after extraction processes, with assignment of T- and Q-type silicon atoms.

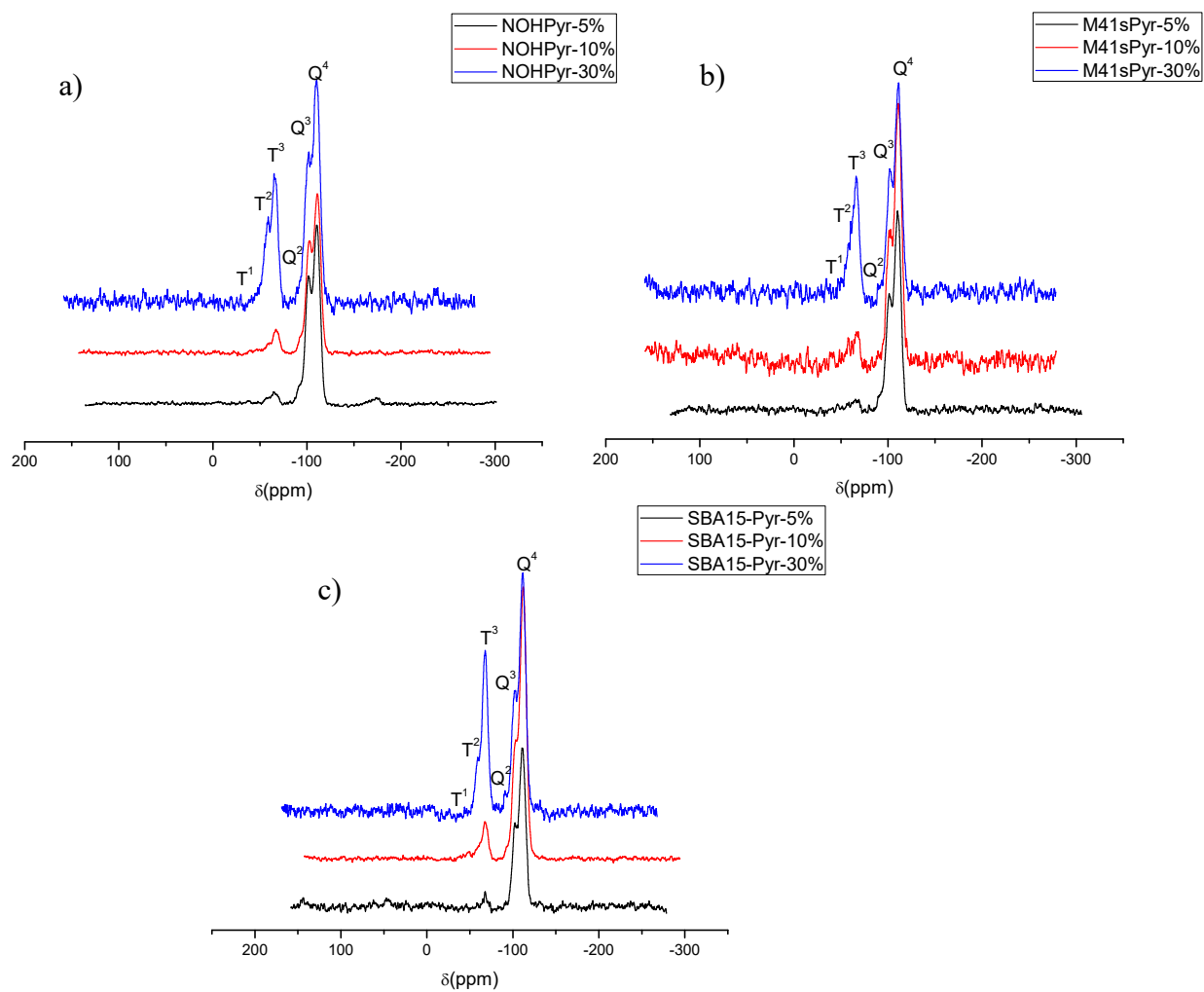


Figure S4. ^{29}Si BD/MAS NMR spectra of (a) NOH-Pyr, (b) M41S-Pyr and (c) SBA-15-Pyr materials, containing different content of bis-silylated pyrrolidine fragments, obtained after extraction processes, with assignment of T- and Q-type silicon atoms.

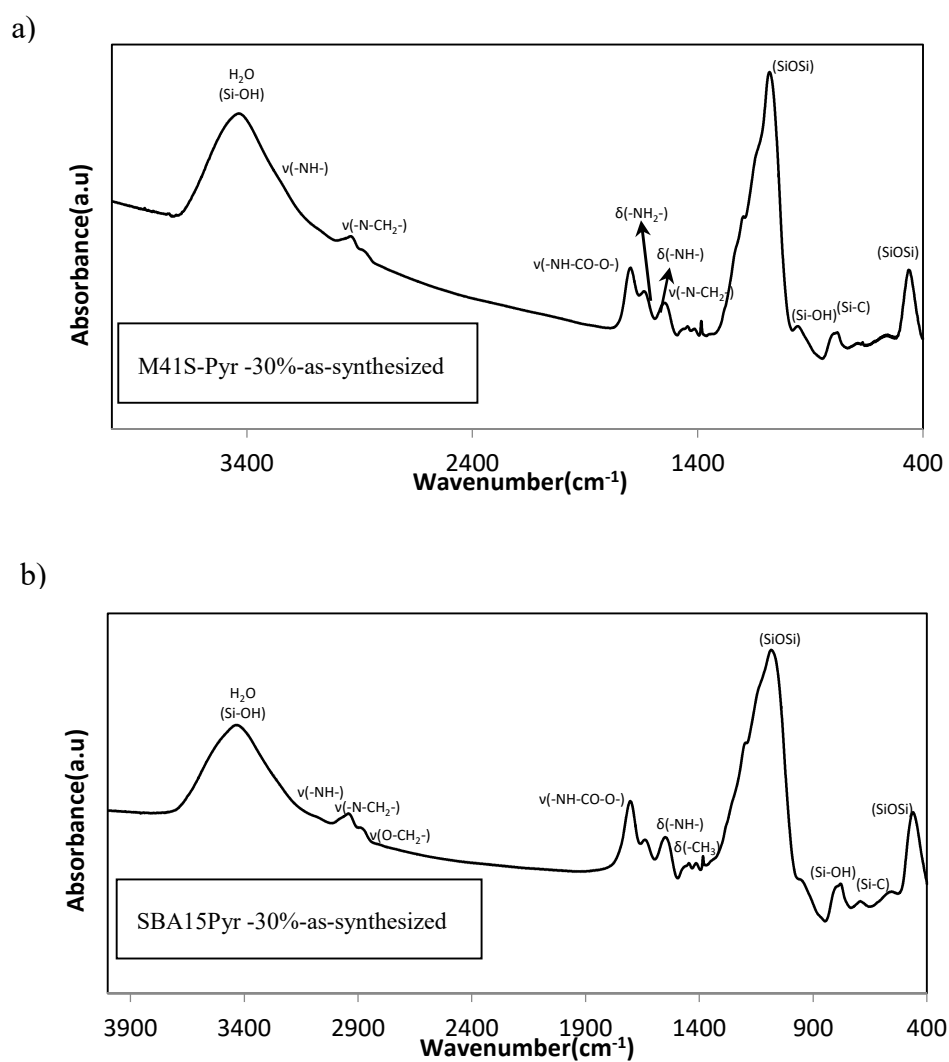
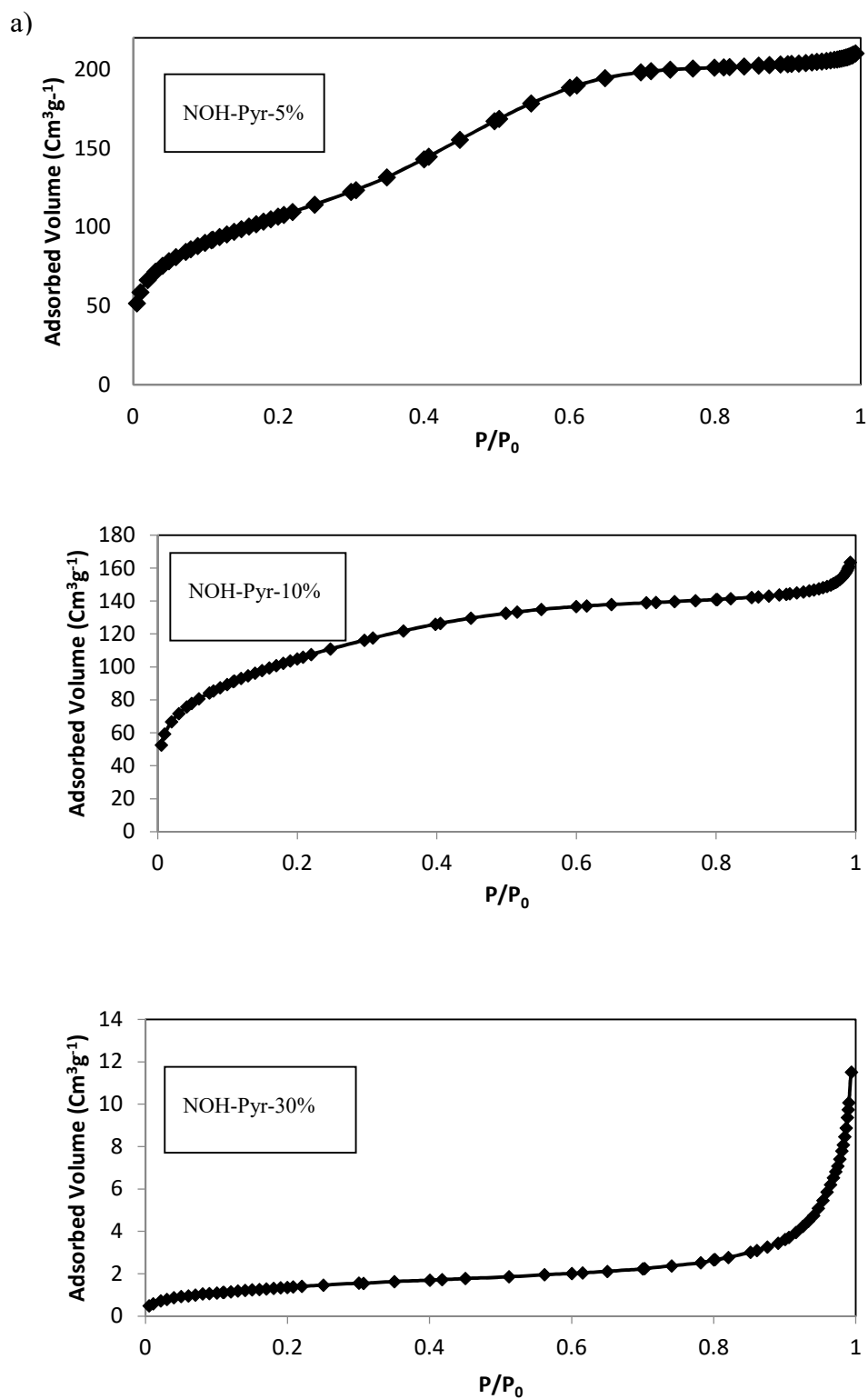
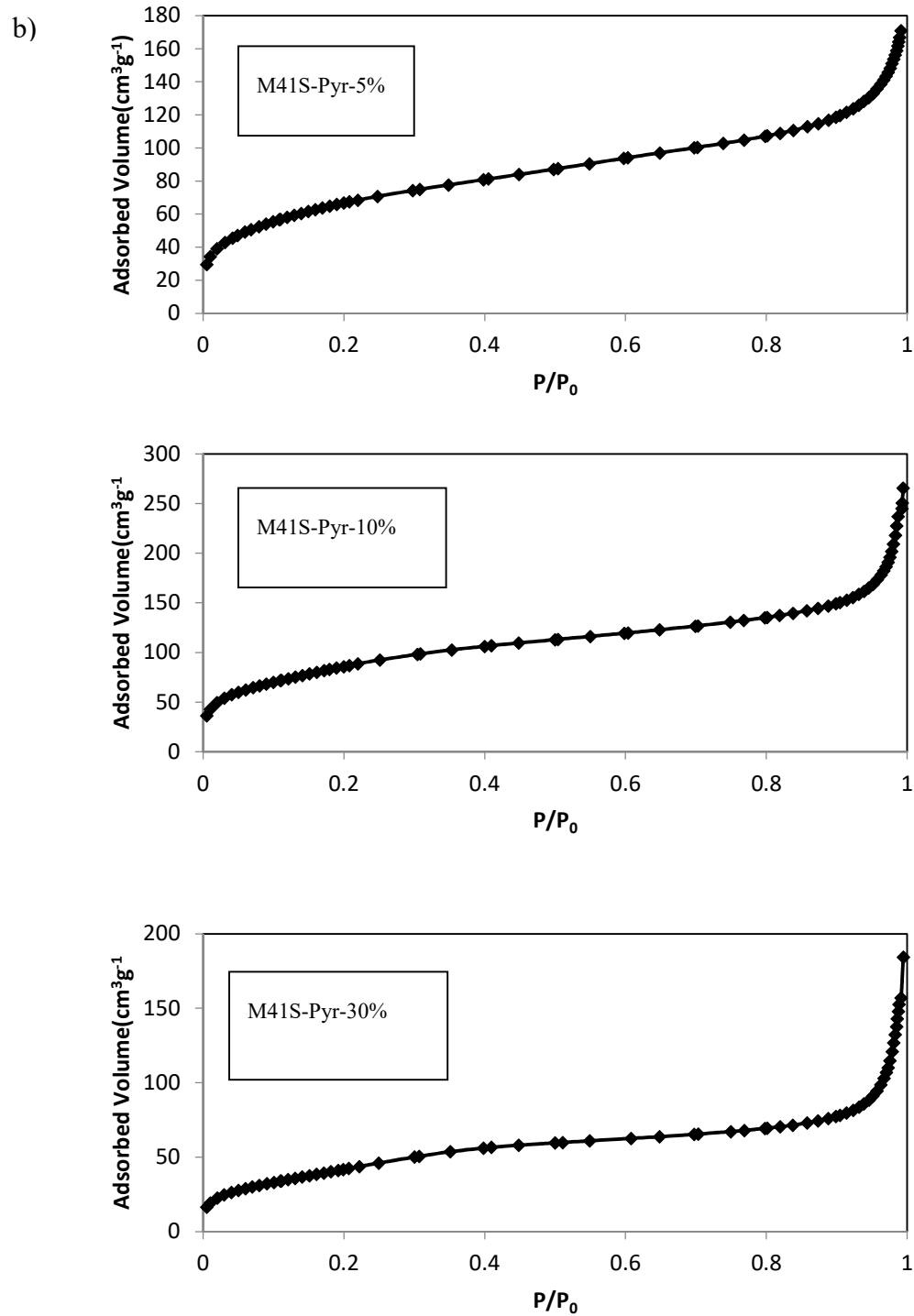


Figure S5. FTIR spectra of as-synthesized (a) M41S-30% and (b) SBA-15-Pyr-30% hybrid materials.





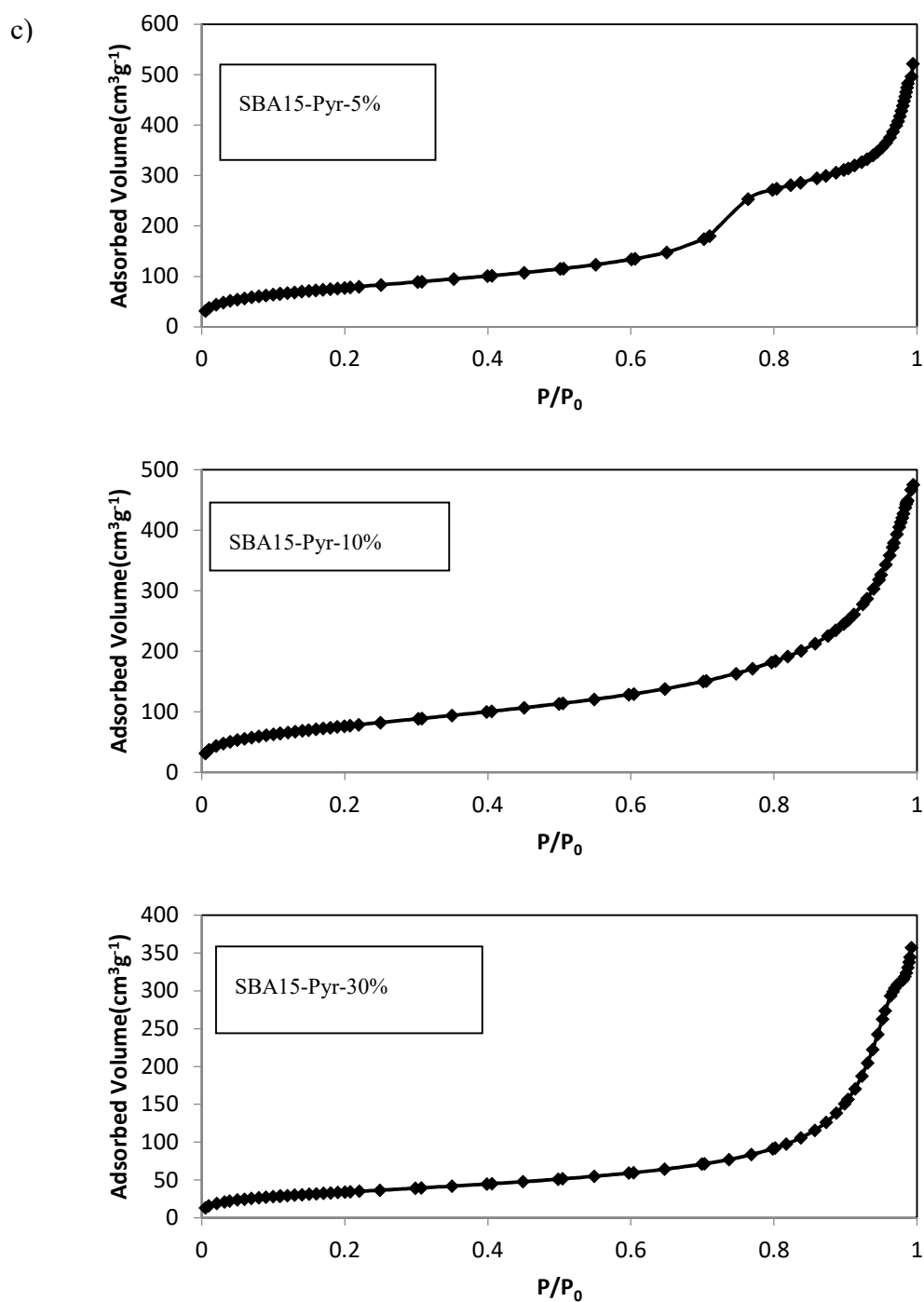


Figure S6. N_2 adsorption isotherms of (a) NOH-Pyr, (b) M41S-Pyr and (c) SBA-15-Pyr materials, containing different content of bis-silylated pyrrolidine fragments, obtained after extraction processes.

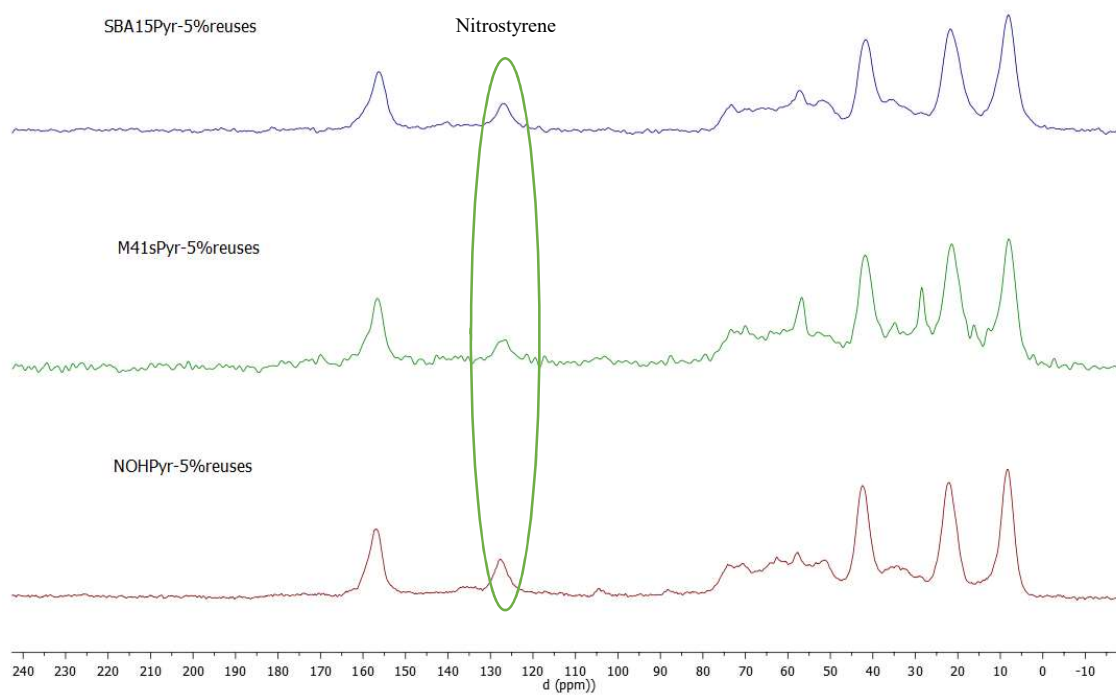


Figure S7. ^{13}C NMR spectra of the different hybrid materials after four/five uses.

Table S1. Integration of T-type and Q-type silicon atoms into the different catalysts obtained after extraction processes.

Catalyst	T ¹	T ²	T ³	Q ²	Q ³	Q ⁴
NOH-Pyr-5%	0.00	0.01	0.03	0.04	0.37	0.56
NOH-Pyr-10%	0.01	0.02	0.07	0.04	0.27	0.54
NOH-Pyr-30%	0.02	0.07	0.22	0.03	0.23	0.45
M41S-Pyr-5%	0.00	0.01	0.03	0.03	0.30	0.54
M41S-Pyr-10%	0.00	0.01	0.03	0.01	0.28	0.79
M41S-Pyr-30%	0.02	0.09	0.20	0.04	0.24	0.41
SBA-15-Pyr-5%	0.00	0.01	0.02	0.01	0.35	1.05
SBA-15-Pyr-10%	0.01	0.02	0.07	0.01	0.21	0.53
SBA-15-Pyr-30%	0.01	0.05	0.28	0.02	0.17	0.47

Table S2. Catalytic results achieved in the presence of the different hybrid materials during several reaction cycles for the enantioselective Michael addition.

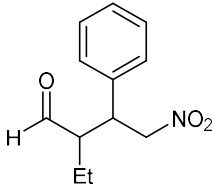
Run	Yield(%)	ee%	dr
<i>NOH-Pyr-5%</i>			
1	96	82%	92:8
2	90	82%	92:8
3	87	82%	90:10
4	89	82%	90:10
5	83	82%	90:10
<i>M41S-Pyr-5%</i>			
1	90	78%	91:9
2	86	78%	91:9
3	82	76%	91:9
<i>SBA-15-Pyr-10%</i>			
1	90	78%	91:9
2	86	78%	91:9
3	82	76%	91:9
4	70	78%	91:9

Table S3. Elemental analysis and C/N molar ratios for NOH-Pyr, M41S-Pyr and SBA-15-Pyr hybrid materials after extraction process and each run.

Run	Catalyst	C%	N%	C/N
0	M41S-Pyr-5%	6.1	1.4	5.0
1	M41S-Pyr-5%	7.1	1.4	5.7
2	M41S-Pyr-5%	7.5	1.4	6.4
3	M41S-Pyr-5%	8.0	1.4	6.7
0	SBA-15-Pyr-10%	10.6	2.6	4.8
1	SBA-15-Pyr-10%	10.7	2.5	5.0
2	SBA-15-Pyr-10%	12.6	2.5	6.0
3	SBA-15-Pyr-10%	13.3	2.4	6.6
0	NOH-Pyr-5%	5.1	1.3	4.6
1	NOH-Pyr-5%	4.9	1.2	4.8
2	NOH-Pyr-5%	6.7	1.5	5.1
3	NOH-Pyr-5%	7.6	1.6	5.5
4	NOH-Pyr-5%	6.8	1.3	6.6

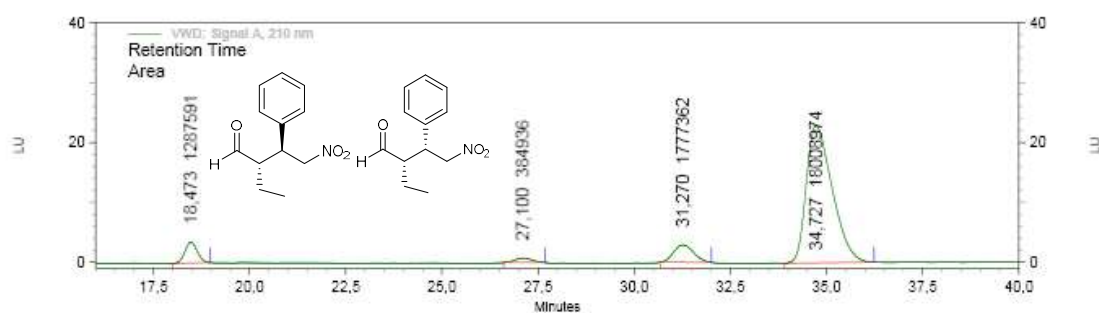
HPLC data

High performance liquid chromatography (HPLC) was performed on an Agilent Technologies chromatograph (1220 Series), using Daicel Chiralpak IC column (4.6 x 250mm).

Product	n-Hexane/ <i>i</i> -PrOH	Flow rate [mL/min]	λ [nm]	tr[<i>min</i>]
	90:10	1.0	210	<i>anti</i> : 18.3, 27.0 <i>syn</i> : 31.2, 35.0

Racemic and chiral HPLC chromatogram for Michael adduct

(2*R*,3*S*)-2-ethyl-4-nitro-3-phenylbutanal

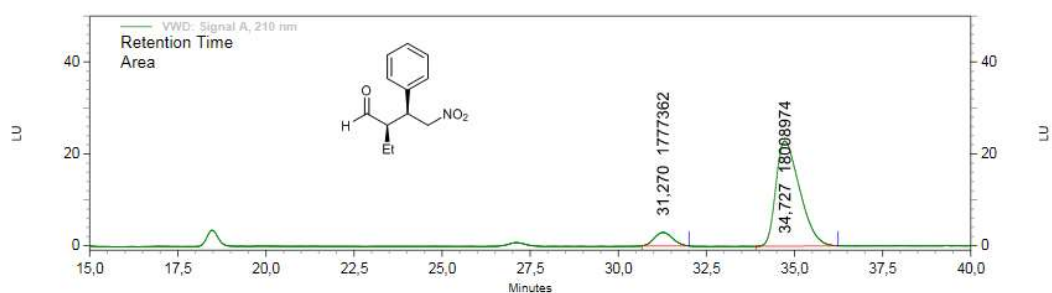


VWD: Signal A, 210 nm

Results

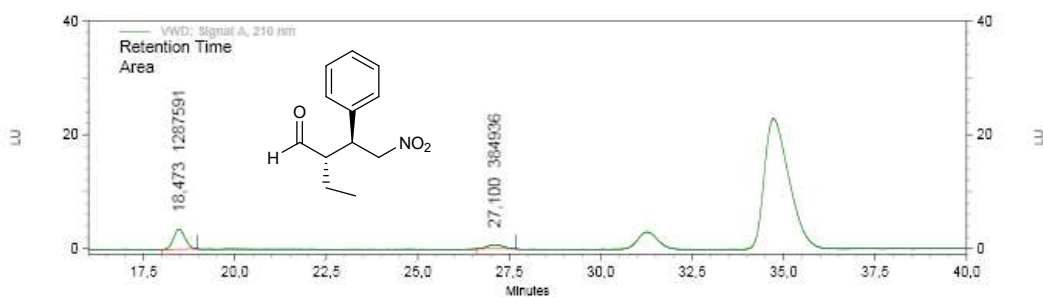
<i>PK</i> #	Retention Time	Area	Area Percent
1	18,473	1287591	6,000
2	27,100	384936	1,794
3	31,270	1777362	8,283
4	34,727	18008974	83,923

Totals		21458863	100,000
--------	--	----------	---------



VWD: Signal A, 210 nm Results

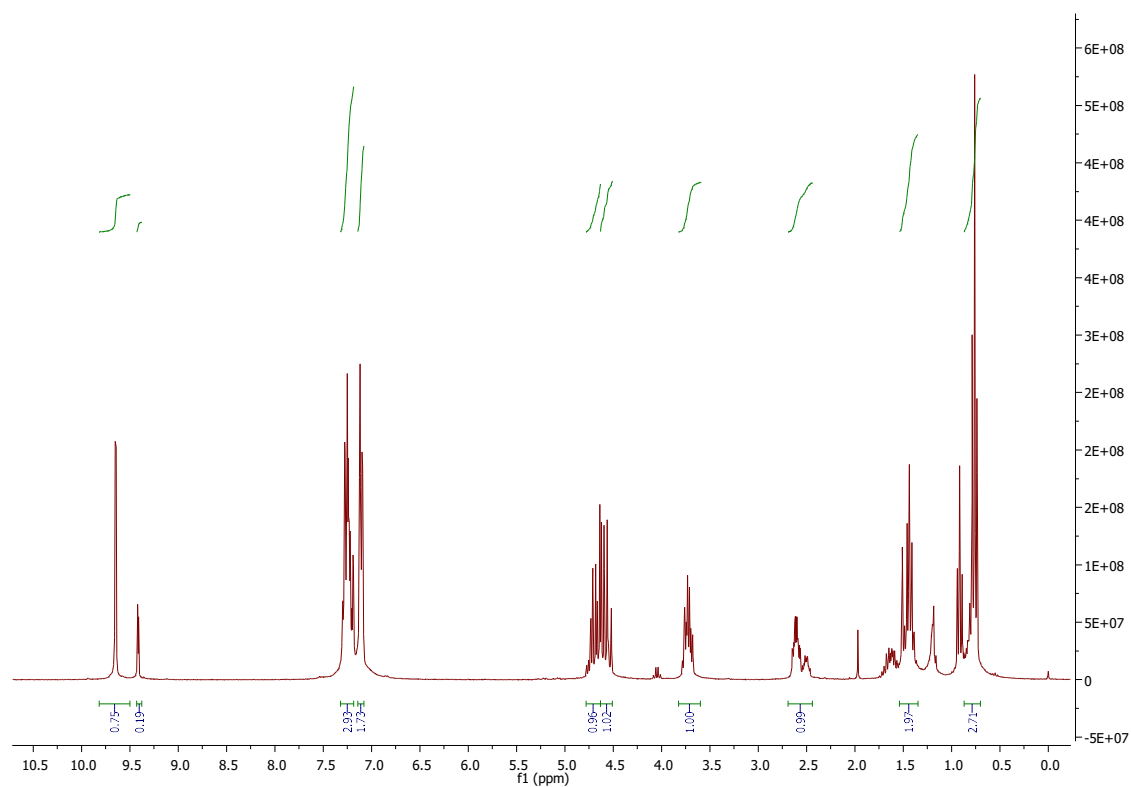
<i>Pk #</i>	<i>Height</i>	<i>Retention Time</i>	<i>Area</i>	<i>Area Percent</i>
1	49086	31,270	1777362	8,983
2	384239	34,727	18008974	91,017
Totals			19786336	100,000



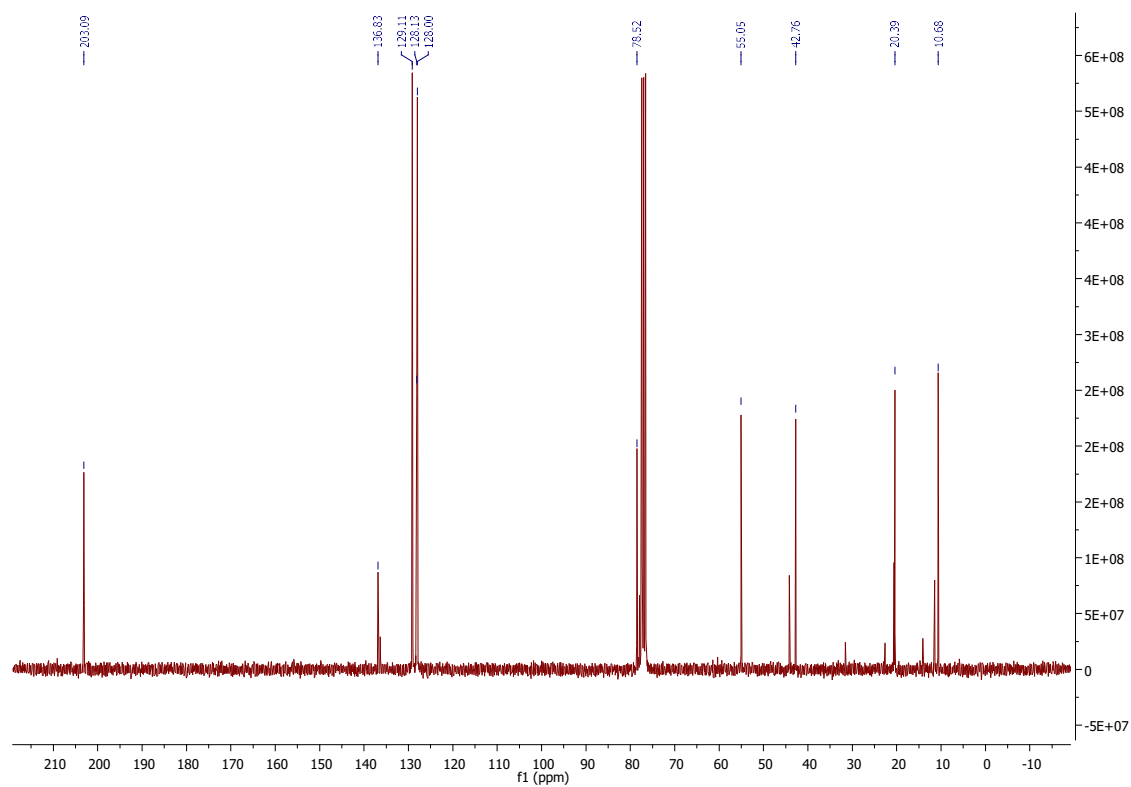
VWD: Signal A, 210 nm Results

<i>Pk #</i>	<i>Retention Time</i>	<i>Area</i>	<i>Area Percent</i>
1	18,473	1287591	76,985
2	27,100	384936	23,015
Totals		1672527	100,000

and

^1H and ^{13}C NMR spectra of Michael adduct

^1H NMR (300 MHz, CDCl_3) δ 9.65 (d, $J = 2.6$ Hz, 1H), 7.31 – 7.18 (m, 3H), 7.11 (m, 2H), 4.70 (dd, $J = 10.8, 5.4$ Hz, 1H), 4.60 (dd, $J = 12.9, 9.3$ Hz, 1H), 3.72 (dt, $J = 9.6, 5.2$ Hz, 1H), 2.61 (dddd, $J = 9.9, 7.6, 5.3, 2.6$ Hz, 1H), 1.54 – 1.37 (m, 3H), 0.76 (t, $J = 7.5$ Hz, 1H).



¹³C NMR (75 MHz, CDCl₃) δ 203.1, 136.9, 129.1 (x2), 128.1, 128.00 (x2), 78.5, 55.1, 42.8, 20.4, 10.7.



© 2018 by the authors. Submitted for possible open access publication under the terms and conditions of the Creative Commons Attribution (CC BY) license (<http://creativecommons.org/licenses/by/4.0/>).